

Bounds on antineutrinos and sterile neutrinos from SNO and SuperKamiokande data

João Pulido and Bhag C. Chauhan ^a

^aCentro de Física Teórica das Partículas,
Departamento de Física, Instituto Superior Técnico
Av. Rovisco Pais, P-1049-001 Lisboa, Portugal

The data from SNO and SuperKamiokande are used to derive upper bounds on antineutrinos $\bar{\nu}_X$ and sterile neutrinos ν_S which may accompany the LMA effect. We consider separately LMA+ $\bar{\nu}_X$, LMA+ ν_S and the general case LMA+ $\bar{\nu}_X$ + ν_S . We obtain for LMA+ $\bar{\nu}_X$ upper and lower bounds on f_B , the SSM normalization factor. For LMA+ ν_S we recover the ν_S upper bound existing in the literature. In the general case it is seen that the upper bound on ν_S is hardly sensitive to the $\bar{\nu}_X$ component. We conclude with a simple χ^2 analysis of all four cases considered.

We perform in this work a model independent analysis of the implications from the SNO salt phases I and II [1] and SuperKamiokande results [2] on the flux of sterile neutrinos and active antineutrinos ν_S , $\bar{\nu}_X$ which may accompany the LMA effect. All results derived for antineutrinos would also apply to $\bar{\nu}_e$ if not for their strict upper bound from the KamLAND experiment [3]. Our analysis is model independent and focuses only on solar neutrino data and its consequences.

We start with the event rate expressions for the charged current (CC) and neutral current (NC) reactions for SNO and neutrino electron scattering (ES) for SK, SNO.

$$R^{CC} = f_B P_{ee} \quad (1)$$

$$R^{NC} = f_B P_{ee} + f_B (1 - P_{ee}) [\sin^2 \alpha s \sin^2 \psi + \bar{r}_d \sin^2 \alpha \cos^2 \psi] \quad (2)$$

$$R^{ES} = f_B P_{ee} + f_B (1 - P_{ee}) [r \sin^2 \alpha \sin^2 \psi + \bar{r} \sin^2 \alpha \cos^2 \psi] \quad (3)$$

Parameter f_B denotes the normalization to the standard solar model 8B neutrino flux [4]. Quantities r , \bar{r} are respectively the ratios of the NC neutrino and antineutrino event rates to the NC+CC neutrino event rate and \bar{r}_d is the ratio of the antineutrino deuteron fission to neutrino deuteron fission event rate. Without loss of generality this is schematically shown in fig.1.

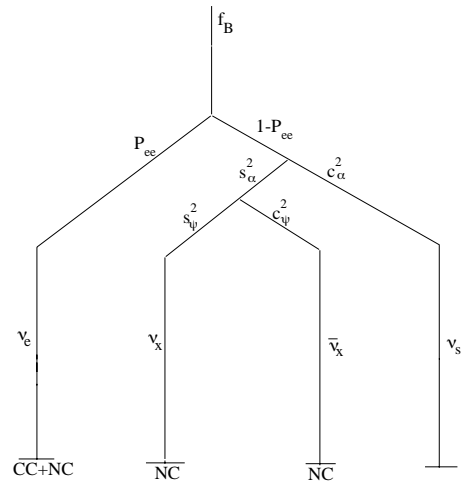


Fig.1 A scheme of LMA as accompanied by antineutrinos and sterile neutrinos.

Denoting by f the energy resolution function and using standard notation, one has

$$r = \frac{\int dE_\nu \phi(E_\nu) \int dE_e \int dE'_e \frac{d\sigma_{NC}}{dE_e} f(E'_e, E_e)}{\sigma_{NC} \rightarrow \sigma_{NC+CC}} \quad (4)$$

with ($r=0.150, 0.151$ for SNO, SK respectively) and a similar equation for \bar{r} with the replacement $\sigma_{NC} \rightarrow \bar{\sigma}_{NC}$. Likewise $\bar{r} = 0.115$ (0.116 for

SK). Energy thresholds considered are $E_{eth}=5.5$, 5 MeV for SNO, SK respectively. For \bar{r}_d one has

$$\bar{r}_d = \frac{\int dE_\nu \phi(E_\nu) \bar{\sigma}_{NC}(E_\nu)}{\bar{\sigma}_{NC} \rightarrow \sigma_{NC}} = 0.954. \quad (5)$$

The survival probability P_{ee} is nearly energy independent in the SNO, SK range, so it factorizes out of these integrals. Thus eqs.(1)-(3) are obtained.

It is possible to eliminate the angle α from eqs.(1)-(3) and relate angle ψ to the experimental quantities R^{CC} , R^{NC} , R^{ES} . The result is

$$\sin^2 \psi = \frac{\bar{r} - \gamma \bar{r}_d}{\gamma(1 - \bar{r}_d) + \bar{r} - r} \quad (6)$$

with

$$\gamma = \frac{R^{ES} - R^{CC}}{R^{NC} - R^{CC}}. \quad (7)$$

The proportions of the $(\nu_X, \bar{\nu}_X)$ in the active non- ν_e flux (parametrized by ψ) are therefore independent of the ν_S component $\cos^2 \alpha$ (see fig.1). If not for the large uncertainties that are propagated into eq. (7), originated from the uncertainties in R^{ES} , R^{CC} , R^{NC} , these proportions would thus be unambiguously determined. Instead, in actual fact, only an upper bound can be obtained for $\sin^2 \psi$. To this end we use eqs. (6), (7) to compute $\sin^2 \psi$ for all values of R^{ES} , R^{CC} , R^{NC} within their allowed 1σ ranges for SNO [1]: this is represented by the light shaded areas in fig.2 where the SNO data used are those from salt phase II. Hence for each chosen value of $\sin^2 \psi$ the allowed values of the three reduced rates lie within each shaded area. If the SNO experiment alone is considered, it is seen that all possible values of $\sin^2 \psi$ in the range $0 \leq \sin^2 \psi \leq 1$ can be obtained. The data from the SK experiment [2] with R^{ES} restricted to its SK 1σ range (see table I) are also used to evaluate $\sin^2 \psi$. The fact that [1] $R^{ES} = 0.368 \pm_{0.050}^{0.056}$ for SNO II while for SK the error bar is much smaller [2], $R^{ES} = 0.406 \pm_{0.011}^{0.013}$, provides the possibility of obtaining a lower limit for $\sin^2 \psi$ (see the dark shaded area in fig.2):

$$\sin^2 \psi > 0.12 \text{ (SNO II) (95\% CL)}. \quad (8)$$

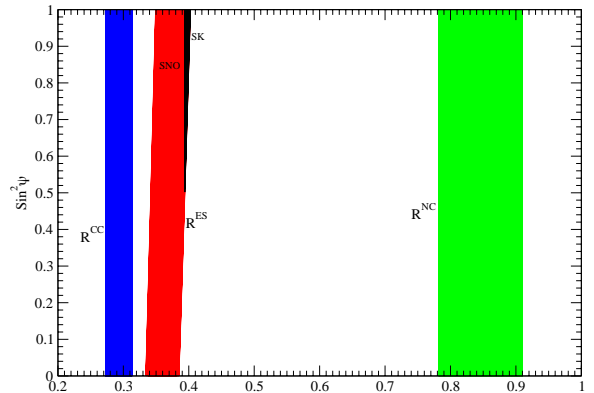


Fig.2 Light shaded areas denote the regions allowed by the 1σ ranges of the reduced rates, as reported by the SNO II experiment, and $\sin^2 \psi$ proportional to the neutrino component of the active non- ν_e flux. The dark shaded area is the region allowed jointly by the SNO II and SK data on the electron scattering reduced rate.

For SNO I [1] $R^{ES} = 0.382 \pm_{0.048}^{0.056}$ implying $\sin^2 \psi > 0.36$ (95% CL). This is an upper bound on the $\bar{\nu}_X$ fraction ($\cos^2 \psi$) of the $(\nu_X, \bar{\nu}_X)$ flux. It is independent of f_B and the ν_S component.

Next we consider the bound on the sterile neutrino flux, proportional to $\cos^2 \alpha$. To do so we must take the general case (LMA+ $\bar{\nu}_X + \nu_S$), since, as opposed to the previous one, the angle ψ cannot be eliminated from eqs. (1)-(3). We have

$$f_B = R^{CC} + \frac{R^{NC} - R^{CC}}{\sin^2 \alpha (\sin^2 \psi + \bar{r}_d \cos^2 \psi)} \quad (9)$$

derived from eqs. (1), (2). This relation is shown in fig.3 as a plot in the $(f_B, \sin^2 \alpha)$ plane for R^{CC} and R^{NC} within their 1σ ranges and the $\bar{\nu}_X$ component up to its 95%CL upper limit. In fig.3 the full lines denote these upper limits [$\cos^2 \psi = 0.88$ for SNO II, $\cos^2 \psi = 0.64$ for SNO I, as seen from eq.(8)] while the dashed lines denote $\cos^2 \psi = 0$ (no $\bar{\nu}_X$). The closeness of the dashed and full lines shows that the possible sterile neutrino flux is hardly sensitive to the presence of antineutrinos: $\cos^2 \psi$ may decrease all the way from 0.88 (0.64) to zero while the sterile flux is almost unaffected. This is because the coefficient of $\sin^2 \alpha$ in eq.(11) is very close to unity

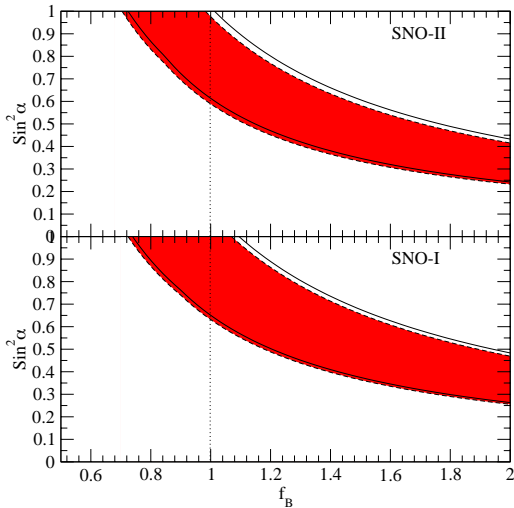


Fig.3 The allowed range at 2σ of $\sin^2\alpha$ (proportional to the total active non- ν_e flux) and f_B , the SSM normalization factor, using SNO II and SNO I data. Dashed lines correspond to absence of antineutrinos, while full lines to their upper bound at 2σ . It is seen that the sterile component, proportional to $\cos^2\alpha$, is hardly affected by the presence of antineutrinos.

$$\bar{r}_d = 0.954 \quad (10)$$

being therefore almost independent of ψ .

We now take an alternative view by considering separately the cases in which either only $\bar{\nu}_X$ or ν_S is present along with LMA and derive in each the corresponding constraints on the SSM normalization factor f_B . We start with the case where no steriles are present (only $\bar{\nu}_X$). Here $\sin^2\alpha = 1$ and from eqs.(2), (3) one obtains

$$f_B = R^{CC} + A \quad (11)$$

with

$$A = \frac{(R^{NC} - R^{CC})(r - \bar{r}) - (R^{ES} - R^{CC})(1 - \bar{r}_d)}{\bar{r}_d(r - \bar{r}) - \bar{r}(1 - \bar{r}_d)} \quad (12)$$

which for SNO II and SNO I give respectively, using table I (to 1σ)

$$f_B = 0.86 \pm 0.12 \text{ (SNO II)} \quad (13)$$

$$f_B = 0.88 \pm 0.13 \text{ (SNO I)}. \quad (14)$$

We note that these correspond to the allowed ranges within the lines $\sin^2\alpha = 1$ in the two panels of fig.3, the slight discrepancies with this figure

being of course the result of the experimental uncertainties and the different procedures used for generating the two sets of results. For the combined SNO and SK data, eqs.(13), (14) become instead (to 1σ)

$$f_B = 0.80 \pm 0.09 \text{ (SNO II + SK)} \quad (15)$$

$$f_B = 0.84 \pm 0.10 \text{ (SNO I + SK)}, \quad (16)$$

the smaller error resulting from the smaller SK error. All these parameter ranges lie within the allowed 1σ SSM error of 23% [4]. It is thus seen that the former general analysis which includes antineutrinos and steriles, and whose results are summarized in fig.3, leads to more precise predictions for f_B , as only two experimentally measured quantities R^{NC} and R^{CC} are used in contrast to eqs.(11), (12). In fact, in fig.3, where all quantities are allowed to vary within their 2σ ranges, we have (for $\sin^2\alpha = 1$)

$$f_B = 0.87 \pm 0.15 \text{ (SNO II)} \quad (17)$$

$$f_B = 0.91 \pm 0.19 \text{ (SNO I)} \quad (18)$$

to be compared with eq.(13), (14) where only 1σ ranges are allowed.

We now briefly refer to the other special case, namely the absence of antineutrinos: only steriles are present here along with the LMA effect, hence $\sin^2\psi = 1$. This case corresponds to the shaded areas in fig.3 limited by the two dashed lines and, in contrast to the previous one, no model independent equation can be obtained for f_B , but only a degeneracy relation between f_B and $\sin^2\alpha$. This can be expressed by the equation

$$f_B = R^{CC} + \frac{R^{NC} - R^{CC}}{\sin^2\alpha} \quad (19)$$

which corresponds to eq.(9) with $\sin^2\psi = 1$. As previously discussed in the general case (LMA + $\bar{\nu}_X + \nu_S$) the main result here is an upper bound on the sterile component. At 2σ this is $\cos^2\alpha < 0.41$ (from SNO II) or 0.38 (from SNO I) of the non- ν_e flux for $f_B = 1$.

We refine our results by performing a χ^2 analysis of all four cases considered. The χ^2 definition is quite simple

$$\chi^2 = \sum_i \frac{(R_i - R_i^{th})^2}{\delta R_i^2} \quad (20)$$

where the sum extends over the four experiments ($i = ES_{SK}, ES_{SNO}, NC, CC$), R_i , δR_i denote the experimental reduced rates and their errors quoted in table I, and R_i^{th} are given by eqs. (1)-(3). The result of the χ^2 minimization is shown in tables I, II for SNO II and SNO I respectively.

	f_B	P_{ee}	$\sin^2\alpha$	$\sin^2\psi$	χ_{min}^2
(i)	0.876	0.356	1.0	1.0	1.67
(ii)	0.876	0.356	1.0	1.0	1.67
(iii)	0.961	0.324	0.869	1.0	1.67
(iv)	0.989	0.315	0.833	1.0	1.67

Table I - Results of χ^2 analysis for SNO II: (i) LMA (2 dof), (ii) LMA+ $\bar{\nu}_x$ (1 dof), (iii) LMA+ ν_s (1 dof), (iv) LMA+ $\bar{\nu}_x + \nu_s$ (2 dof).

Inspection of table I (second row) shows that the best fit for case LMA+ $\bar{\nu}_X$ corresponds to the very absence of $\bar{\nu}_X$ ($\sin^2\psi = 1$). It is also seen that allowing for ν_S alone in addition to LMA (third row) as well as LMA+ $\bar{\nu}_X + \nu_S$ (fourth row) leads to a best fit solution with a small although non negligible ν_S component (13% and 17% respectively). Furthermore table I also shows that χ_{min}^2 is independent of the values of f_B , P_{ee} , $\sin^2\alpha$. However it depends on $\sin^2\psi$: if in fact we let $\sin^2\psi$ to be unconstrained, an absolute χ_{min}^2 is obtained for an unphysical value of $\sin^2\psi$,¹. As long as $\sin^2\psi$ remains constrained to its physical region ($0 \leq \sin^2\psi \leq 1$), χ_{min}^2 is fixed regardless of the values of the other three parameters f_B , P_{ee} , $\sin^2\alpha$. A similar situation is observed in SNO I (see table II) with the sterile component totally missing ($\sin^2\alpha = 1$) in the LMA+ ν_S case. This reflects the fact that the parameters f_B , P_{ee} , $\sin^2\alpha$ can be eliminated from eqs.(1)-(3) so as to express $\sin^2\psi$ ($\bar{\nu}_X$ component) in terms of experimentally measured quantities only (see eqs. (6), (7)). Likewise the bound on $\sin^2\psi$ is independent of the ν_S component and of the other two parameters f_B , P_{ee} [see eq. (8)].

¹These are $\chi_{min}^2 = 0.384$, $\sin^2\psi = 2.84$ (SNO II) and $\chi_{min}^2 = 0.133$, $\sin^2\psi = 3.17$ (SNO I).

	f_B	P_{ee}	$\sin^2\alpha$	$\sin^2\psi$	χ_{min}^2
(i)	0.965	0.304	1.0	1.0	2.47
(ii)	0.965	0.304	1.0	1.0	2.47
(iii)	0.965	0.304	1.0	1.0	2.47
(iv)	0.969	0.302	0.933	1.0	2.47

Table II - Same as Table I for SNO I.

To conclude:

(i) We found an upper bound for $\bar{\nu}_X$ which at 2σ is 0.88 (SNO II) or 0.64 (SNO I) of the active non- ν_e flux [see fig.2 and eq.(8)]. This is independent of the sterile neutrino component.

(ii) In the no sterile case we obtained upper and lower bounds on f_B [eqs.(13)-(18)].

(iii) In the no $\bar{\nu}_X$ case (only steriles accompanying LMA) the fraction of solar neutrinos oscillating to active ones was found to be greater than 0.59 (SNO II) or 0.63 (SNO I) of the non- ν_e flux, a result consistent with ref. [5] which is in fact an upper bound on ν_S .

(iv) Allowing, in the preceding situation, for $\bar{\nu}_X$ up to its 2σ upper bound, these limits are increased by only 5%, (decrease on ν_S upper bound) which shows how the possible ν_S flux is hardly sensitive to the $\bar{\nu}_X$ component.

(v) χ^2 analysis shows that the most disfavoured case (if not excluded) is $\bar{\nu}_X$ either with LMA or with LMA+ ν_S . In SNO II it is seen that some possibility is left for LMA+ ν_S .

REFERENCES

1. S. N. Ahmed *et al.* [SNO Collaboration], Phys. Rev. Lett. **92**, 181301 (2004).
2. S. Fukuda *et al.* [Super-Kamiokande Collaboration], Phys. Lett. B **539**, 179 (2002).
3. K. Eguchi *et al.* [KamLAND Collaboration], Phys. Rev. Lett. **92**, 071301 (2004).
4. J. N. Bahcall and M. H. Pinsonneault, Phys. Rev. Lett. **92**, 121301 (2004).
5. A. B. Balantekin, V. Barger, D. Marfatia, S. Pakvasa and H. Yuksel, arXiv:hep-ph/0405019.